Title

Golgi Outposts Shape Dendrite Morphology by Functioning as Sites of Acentrosomal Microtubule Nucleation in Neurons

Authors

Ori-McKenney, Kassandra M
Jan, Lily Yeh
Jan, Yuh-Nung

Golgi outposts shape dendrite morphology by functioning as sites of acentrosomal microtubule nucleation in neurons

Kassandra M. Ori-McKenney[1], **Lily Yeh Jan**[1], and **Yuh-Nung Jan**[1,*]
[1]Howard Hughes Medical Institute; Department of Physiology; University of California, San Francisco, CA 94158; USA

SUMMARY

Microtubule nucleation is essential for proper establishment and maintenance of axons and dendrites. Centrosomes, the primary site of nucleation in most cells, lose their function as microtubule organizing centers during neuronal development. How neurons generate acentrosomal microtubules remains unclear. *Drosophila* dendritic arborization (da) neurons lack centrosomes and therefore provide a model system to study acentrosomal microtubule nucleation. Here we investigate the origin of microtubules within the elaborate dendritic arbor of class IV da neurons. Using a combination of *in vivo* and *in vitro* techniques, we find that Golgi outposts can directly nucleate microtubules throughout the arbor. This acentrosomal nucleation requires gamma-tubulin and CP309, the *Drosophila* homologue of AKAP450, and contributes to the complex microtubule organization within the arbor, and dendrite branch growth and stability. Together, these results identify the first direct mechanism for acentrosomal microtubule nucleation within neurons, and reveal a previously unknown function for Golgi outposts in this process.

INTRODUCTION

Microtubules are organized into dynamic arrays that serve as tracks for directed vesicular transport, and are essential for the proper establishment and maintenance of neuronal architecture (Bartolini and Gundersen, 2006; Hoogenraad and Bradke, 2009; Keating and Borisy, 1999; Stiess and Bradke, 2010; Witte and Bradke, 2008). The organization and nucleation of microtubules must be highly regulated in order to generate and maintain such complex arrays (Desai and Mitchison, 1997). Nucleating complexes, in particular, are necessary because spontaneous nucleation of new tubulin polymers is kinetically limiting both *in vivo* and *in vitro* (Oegema et al., 1999). Gamma(γ)-tubulin is a core component of microtubule organization centers and has a well-established role in nucleating spindle and cytoplasmic microtubules (Oakley, 2000). Previous studies have proposed that in mammalian neurons, microtubules are nucleated by γ-tubulin at the centrosome, released by microtubule severing proteins, and then transported into developing neurites by motor proteins (Ahmad et al., 1998; Baas et al., 2005; Wang and Brown, 2002; Yu et al., 1993). Indeed, injection of antibodies against γ-tubulin or severing proteins inhibited axon outgrowth in neurons cultured for one day in vitro (DIV1) (Ahmad et al., 1994; Ahmad et al., 1999).

*Correspondence: yuhnung.jan@ucsf.edu.

However, proper neuron development and maintenance may not rely entirely on centrosomal sites of microtubule nucleation. Although the centrosome is the primary site of microtubule nucleation at DIV2, it loses its function as a microtubule-organizing center during neuronal development (Stiess et al., 2010). In mature cultured mammalian neurons (DIV 11–12), γ-tubulin is depleted from the centrosome, and the majority of microtubules emanate from acentrosomal sites (Stiess et al., 2010). In *Drosophila dsas-4* mutants that lack centrioles, organization of eye-disc neurons and axon outgrowth are normal in 3rd instar larvae (Basto et al., 2006). Within the *Drosophila* peripheral nervous system (PNS), although dendritic arborization neurons contain centrioles, they do not form functional centrosomes, and laser ablation of the centrioles does not perturb microtubule growth or orientation (Nguyen et al., 2011). These results indicate that acentrosomal generation of microtubules contributes to axon development and neuronal polarity. How and where acentrosomal microtubule nucleation may contribute to the formation and maintenance of the more complex dendrites, and what factors are involved in this nucleation is unknown. Dendritic arborization (da) neurons provide an excellent system for investigating these questions. They are a sub-type of multipolar neurons in the PNS of *Drosophila melanogaster*, which produce complex dendritic arrays and do not contain centrosomes (Grueber et al., 2002, 2003; Nguyen et al., 2011). Based on their patterns of dendrite projections, the da neurons have been grouped into four classes (I–IV) with branch complexity and arbor size increasing with class number. Class IV da neurons are ideal for studying acentrosomal microtubule nucleation because they have the most elaborate and dynamic dendritic arbor, raising intriguing questions about the modes of nucleation for its growth and maintenance.

One potential site of acentrosomal microtubule nucleation within these neurons is the Golgi complex. A number of studies have shown that the Golgi complex can nucleate microtubules in fibroblasts (Chabin-Brion et al., 2001; Efimov et al., 2007; Miller et al., 2009; Rivero et al., 2009). Although, in these cell types, the Golgi is tightly coupled to the centrosome, it does not require the centrosome for nucleation. It does however require γ-tubulin, the centrosomal protein AKAP450, and the microtubule binding proteins CLASPs (Chabin-Brion et al., 2001; Efimov et al., 2007; Hurtado et al., 2011; Miller et al., 2009; Rivero et al., 2009). When the Golgi is fragmented upon treatment with nocodazole, the dispersed Golgi ministacks can still promote microtubule nucleation, indicating that these individual ministacks contain the necessary machinery for nucleation (Efimov et al., 2007; Rivero et al., 2009).

In both mammalian and *Drosophila* neurons, the Golgi complex exists as Golgi stacks located within the soma and Golgi outposts located within the dendrites (Gardiol et al., 1999; Horton and Ehlers, 2003; Pierce et al., 2001). In cultured mammalian hippocampal neurons, these Golgi outposts are predominantly localized in a subset of the primary branches (Horton et al., 2005); however, in *Drosophila* class IV da neurons, the Golgi outposts appear throughout the dendritic arbor, including within the terminal branches (Ye et al., 2007). The Golgi outposts may provide membrane for a growing dendrite branch, as the dynamics of smaller Golgi outposts are highly correlated with dendrite branching and extension (Horton et al., 2005; Ye et al., 2007). However, the majority of larger Golgi outposts remains stationary at dendrite branchpoints and could have additional roles beyond membrane supply (Horton et al., 2005; Ye et al., 2007). It is unknown whether *Drosophila* Golgi outposts contain nucleation machinery similar to mammalian Golgi stacks. Such machinery could conceivably support microtubule nucleation within the complex and dynamic dendritic arbor.

In this study, we identify a direct mechanism for acentrosomal microtubule nucleation within the dendritic arbor and reveal a novel role for Golgi outposts in this process. Golgi

outposts contain both γ-tubulin and CP309, the *Drosophila* homologue of AKAP450, both of which are necessary for Golgi outpost-mediated microtubule nucleation. This type of acentrosomal nucleation contributes not only to the generation of microtubules at remote terminal branches, but also to the complex organization of microtubules within all branches of the dendritic arbor. Golgi outposts are therefore important centers of acentrosomal microtubule nucleation, which is necessary to establish and maintain the complexity of the class IV da neuronal arbor.

RESULTS

Microtubule orientation differs in primary *vs.* terminal branches of *Drosophila* class IV dendritic arborization neurons

In order to understand how the microtubule cytoskeleton is organized in the branches of class IV dendritic arborization (da) neurons, we analyzed the dynamics of EB1-GFP comets throughout the entire dendritic arbor *in vivo*. We expressed *UAS-EB1-GFP* using the class IV specific promoter, *ppk-Gal4*, and focused on 3rd instar larvae 96 hours after egg laying, because although the arbor is well established and the primary branches are stable, the terminal branches are still dynamic (Lee et al., 2011; Parrish et al., 2009; Ye et al., 2007). Using EB1-GFP to mark the growing plus ends of microtubules, we found that microtubules grew predominantly in the retrograde direction towards the cell body in long ($> 50\ \mu m$) primary branches, consistent with previous reports in other classes of neurons (Figure 1A) (Mattie et al., 2010; Rolls et al., 2007; Satoh et al., 2008; Song et al., 2012; Stone et al., 2008; Zheng et al., 2008). However, in shorter branches (20–30 μm), we detected mixed microtubule polarity (Figure 1B), similar to that defined in mammalian neurons (Baas et al., 1988; Kapitein et al., 2010). Branches of this length corresponded to higher order branches, such as the secondary and tertiary branches, from which terminal branches originate (Figure S1). In even shorter terminal branches ($< 20\ \mu m$), EB1 comets grew predominantly in the anterograde direction towards the distal tip of the branch (Figure 1C–D). Therefore, microtubule orientation within the dendritic arbor correlates with the length of the dendrite branch. Longer, more established branches contain predominately retrograde EB1 comets and shorter branches are composed of mainly anterograde EB1 comets (Figure 1E). This held true for branches in both the proximal and distal regions of the arbor. The speeds of the anterograde and retrograde comets were comparable in all branches, and closely matched the growth rates of microtubules in other systems (Figure 1F) (Akhmanova et al., 2001; Stepanova et al., 2003).

Microtubules originate from distinct sites within the terminal branches

In order to generate different patterns of microtubule polarity throughout the dendritic arbor, there likely exist a variety of mechanisms for microtubule nucleation. We therefore wanted to understand the origins of anterograde and retrograde EB1 comets growing specifically within the terminal branches. Anterograde comets originated from three main sources: the parent branch (Figure 2A), the branchpoint (Figure 2B), and within the terminal branch (Figure 2C). EB1 comets growing retrogradely along the parent branch could be directed into a smaller daughter branch and grow anterogradely towards the distal tip; however, this was the least common source of EB1 comets for the terminal branches (20% and 5% of anterograde comets in $< 10\ \mu m$ and $> 10\ \mu m$ branches, respectively) (Figure 2A, D–E). Anterograde comets that originated from the branchpoint were most common for branches under 10 μm (58% of comets), while comets that originated within the branch were most common for branches over 10 μm (79% of comets) (Figure 2B–C, D–E, Movie S1). Intriguingly, in both instances, the EB1 comets grew from very specific sites, indicating these microtubules may be nucleated from a common structure located at the branchpoint or within the branch (Figure 2B–C). Though retrograde comets were quite rare in these

terminal branches, we also wanted to understand their origins. Retrograde comets either grew from the distal tip of the branch, which was more common in shorter branches, or within the branch, which was more common in longer branches (Figure 2F, G–H; Figure S2A–C). Again, multiple EB1 comets emanated from the same site, suggesting that these microtubules may be nucleated from specific structures within the branch.

Golgi outposts nucleate microtubules both *in vivo* and *in vitro*

Previous studies have reported that Golgi outposts are often enriched at dendritic branchpoints (Horton et al., 2005; Ye et al., 2007), the most common site for anterograde EB1 comets growing into short terminal branches (Figure 2E). In class IV da neurons, Golgi outposts were located at 47% of branchpoints, but they also appeared throughout the entire dendritic arbor, including at 25% of distal tips (Figure S3A–D). The Golgi complex has been shown to support microtubule nucleation in fibroblasts, and Golgi outposts contain both *cis* and *trans* elements (Horton and Ehlers, 2003). Therefore, we asked whether the Golgi outposts in these da neurons could also be sites of microtubule nucleation within the dendritic arbor. We expressed *UAS-manII-mCherry* to label Golgi outposts (Ye et al., 2007) and *UAS-EB1-GFP* using class IV neuron-specific drivers and noticed a striking correlation between the site of Golgi outposts and the site of EB1 comet formation. We observed that Golgi outposts correlated with EB1 comet formation at dendrite branchpoints (Figure 3A, Movie S2), distal tips (Figure 3B), and within the terminal branch (Figure 3C). Other organelles, such as Rab11-positive endosomes and mitochondria, did not correlate with EB1 comet formation *in vivo* (data not shown). Multiple EB1 comets could originate from a single Golgi outpost, with an average time of 66 sec between formation of the first and second comets. Strikingly, multiple EB1 comets always emanated from the Golgi outposts in a particular direction, suggesting specific polarity in the nucleation machinery, and a role for the outposts in establishing or maintaining microtubule orientation within the terminal branch.

We also wanted to determine if there was a similar correlation within the primary branch, where EB1 comets predominantly move in the retrograde direction and Golgi outposts are rapidly transported (Golgi outposts moved at an average speed of 0.8 μm/sec compared with the EB1 comet growth speed of 0.1 μm/sec; Figure S3E). Even in primary branches, stationary Golgi outposts colocalized with sites of EB1 comet formation, and again, all of the EB1 comets grew specifically in the retrograde direction (Figure 3D). The population of rapidly transported outposts did not colocalize with EB1 comet origins; however, we did observe that some moving outposts became stationary followed by nucleation of EB1 comets (Figure 3A, D). Overall, we observed 45% of total EB1 comets originating from Golgi outposts and 44% of total Golgi outposts correlating with EB1 comet formation (Figure 3E–F). These results strongly support a role for Golgi outposts as microtubule nucleation sites within da neurons.

We next asked whether these Golgi outposts could support microtubule nucleation *in vitro*. We partially purified Golgi vesicles from *ppk-Gal4>UAS-ManII-eGFP* fly embryos. We separated the vesicles from other membranous structures via vesicle flotation through a sucrose step gradient, and then tested the ability of these vesicles to nucleate microtubules when incubated with purified tubulin and GTP (Hendricks et al., 2010; Kollman et al., 2010; Macurek et al., 2008; Mitchison and Kirschner, 1984; Ori-McKenney et al., 2010). We observed numerous microtubules extending from GFP-labeled Golgi vesicles, indicating that these vesicles are competent to promote microtubule nucleation *in vitro* (Figure 4A–D). Quantification revealed that 54% of the GFP-labeled Golgi vesicles were associated with one or more microtubules, and 60% of the microtubules extended from Golgi vesicles, consistent with our *in vivo* results (Figure 4A–C). To investigate the differences between the Golgi vesicles that could support nucleation and those that could not, we immunostained the

vesicles for γ-tubulin and CP309, the *Drosophila* homologue of AKAP450 (Figure 4B–C) (Kawaguchi and Zheng, 2004). Both proteins were present on the Golgi outpost vesicles associated with microtubules. Strikingly, 85% of the γ-tubulin positive vesicles and 68% of the CP309 positive vesicles nucleated microtubules (Figure 4D). In contrast, we did not observe microtubule nucleation from any of the γ-tubulin negative vesicles. We were also able to inhibit microtubule nucleation from Golgi vesicles with a γ-tubulin function blocking antibody (Figure S4) (Joshi et al., 1992). Together these results reveal that Golgi outposts are novel sites of microtubule nucleation both *in vivo* and *in vitro*, and that this activity requires γ-tubulin and CP309.

γ-tubulin and CP309 are necessary for Golgi outpost-mediated microtubule nucleation *in vivo*

Next, we asked whether γ-tubulin and CP309 were essential for microtubule nucleation by Golgi outposts *in vivo*. We combined the *UAS-γ-tubulin-23C* RNAi with the loss of function allele, *γ-tubulin-23C$^{(A15-2)}$*, to generate viable mutant larvae with a robust phenotype. We found a dramatic reduction in the percent of Golgi outposts that correlate with EB1 comet formation, and in the percent of EB1 comets emanating from Golgi outposts in neurons of these γ-tubulin mutants as well as *CP309$^{(5)}$/CP309$^{(5)}$* loss of function mutant larvae (Figure 5A–B). Interestingly, the Golgi outposts were still localized to branchpoints and scattered throughout the arbor in both mutants (Figure 5C). The number of EB1 comets was also unchanged in the primary branches; however, there were fewer comets entering the terminal branches of these mutant neurons (Figure 5D–E). We next examined the neuronal morphology in the absence of Golgi outpost mediated microtubule nucleation. Sholl analysis revealed an overall decrease in the complexity of the arbor of both γ-tubulin and CP309 mutant neurons, with a reduction in total dendrite length and in the number of branchpoints (Figure 6A–E). Remarkably, the terminal branches were most affected, while the primary and secondary branches seemed to develop relatively normally (Figure 6A). Maternally contributed γ-tubulin (*γ-tubulin-37C*) could be necessary for the initial development of the primary arbor, but it is reportedly degraded by the 3rd larval instar (Basto et al., 2006; Wiese and Zheng, 2006). Our data indicate that Golgi outpost associated γ-tubulin-23C could be necessary for the maturation of the rest of the arbor, especially for terminal branch growth.

Microtubules are necessary for the growth and stability of terminal branches within the da neuron arbor

In order to understand how microtubule nucleation could affect terminal branch dynamics, we compared the dynamics of terminal branches that contained EB1 comets with those that did not over the course of 30 min in wild type larval neurons. We found that when EB1 comets entered a terminal branch, the branch either extended or remained stable, and rarely retracted (Figure 7A–B; 40.7 % extended and 7.4 % retracted). On the other hand, the majority of terminal branches that lacked EB1 comets retracted (Figure 7B and Figure S5A–B; 13.6 % extended and 50.8 % retracted). We noticed far fewer EB1 comets entering terminal branches in the γ-tubulin and CP309 mutant neurons (Figure 5E), indicating the ability of a terminal branch to extend or remain stable could be compromised in these mutant neurons. We therefore analyzed the branch dynamics of γ-tubulin and CP309 mutant neurons and indeed found that the terminal branches were less stable than those of wild type neurons, with the majority of the branches retracting (Figure 7C–D; 69% for γ-tubulin mutant and 53% for CP309 mutant *vs.* 34% for wild type). Together these results reveal that γ-tubulin positive Golgi outposts may be especially important at branchpoints for nucleating microtubules into the terminal branches to promote their growth and stability. Without this mechanism of generating microtubules, the terminal branches are deficient in their ability to extend and fill in the arbor (Figure 6A).

DISCUSSION

We have addressed how microtubules are organized and nucleated within the complex arbor of class IV da neurons, and how essential these processes are for dendrite growth and stability. Microtubule organization within different subsets of branches in da neurons must require many levels of regulation. In this current study, we have identified the first direct mechanism for acentrosomal microtubule nucleation within these complex neurons, and uncovered a novel role for Golgi outposts in this process. Our data are consistent with the observation that pericentriolar material is redistributed to the dendrites in mammalian neurons (Ferreira et al., 1993), and that γ-tubulin is depleted from the centrosome in mature mammalian neurons (Stiess et al., 2010). This suggests that the Golgi outposts may be one structure involved in the transport of centriole proteins such as γ-tubulin and CP309. We find that microtubule nucleation from these Golgi outposts correlates with the extension and stability of terminal branches, which is consistent with the observation that EB3 comet entry into dendritic spines accompanies spine enlargement in mammalian neurons (Jaworski et al., 2009). It is striking that microtubule organization in shorter branches, but not primary branches, mimics the organization in mammalian dendrites, with a mixed microtubule polarity in the secondary branches and a uniform plus end distal polarity in the terminal branches (Baas et al., 1988). Kinesin-2 and certain +TIPS are necessary for uniform minus end distal microtubule polarity in the primary dendrites of da neurons (Mattie et al., 2010). Golgi outpost mediated microtubule nucleation could also contribute to establishing or maintaining this polarity both in the terminal branches and in the primary branches. It will be of interest to identify other factors that may be involved in organizing microtubules in different subsets of branches in the future.

Our *in vivo* and *in vitro* data support a role for Golgi outposts in nucleating microtubules at specific sites within terminal and primary branches. However, we note that not all EB1 comets originate from Golgi outposts, indicating other possible mechanisms of generating microtubules (Figure 3) (Rogers et al., 2008). One potentially important source of microtubules is the severing of existing microtubules by such enzymes as katanin and spastin, both of which are necessary for proper neuronal development (Ahmad et al., 1999; Jinushi-Nakao et al., 2007; Stewart et al., 2012; Yu et al., 2008). It is likely that both microtubule nucleation and microtubule severing contribute to the formation of new microtubules within the dendritic arbor; however, our studies suggest that Golgi-mediated nucleation is especially important for the growth and maintenance of the terminal arbor. In γ-tubulin and CP309 mutant neurons, the primary branches contain a similar number of EB1 comets, but only a small fraction of the terminal branches still contain EB1 comets. This result indicates that severing activity or other sources of nucleation may suffice for microtubule generation within the primary branches, but γ-tubulin mediated nucleation is crucial in the terminal branches. As a result, the terminal branch arbor is dramatically reduced by mutations compromising the γ-tubulin nucleation activity at Golgi outposts (Figure 6).

It is important to note that Golgi outposts are present in the dendrites, but not in the axons of da neurons, thus this mode of nucleation is dendrite specific and likely contributes to the difference in microtubule arrays in axons and dendrites. While the axon is one long primary branch with uniform microtubule polarity, the dendrite arbor is an intricate array of branches where microtubule polarity depends on branch length (Figure 1). Therefore, this more elaborate branched structure may have evolved a variety of nucleation mechanisms, including Golgi outpost nucleation and microtubule severing. Intriguingly, in da neurons lacking cytoplasmic dynein function, the Golgi outposts are mislocalized to the axon, which appears branched and contains microtubules of mixed polarity (Zheng et al., 2008). We speculate that in these mutants, Golgi-mediated microtubule nucleation within the axon is

contributing to the mixed microtubule orientation and formation of ectopic dendrite-like branches.

Only a subpopulation of Golgi outposts could support microtubule nucleation both *in vivo* and *in vitro*. Our results show that Golgi outpost mediated microtubule nucleation is restricted to stationary outposts, and dependent upon γ-tubulin and CP309, but why some outposts contain these proteins while others do not is unknown. γ-tubulin and CP309 could be recruited to the Golgi outposts in the cell body and transported on the structure into the dendrites, or they could be recruited locally from soluble pools throughout the dendritic arbor. Golgi outposts are small enough to be trafficked into terminal branches that are 150–300 nm in diameter (Han et al., 2012; Ye et al., 2007), and therefore may provide an excellent vehicle for transporting nucleation machinery to these remote areas of the arbor. It will be interesting to determine how these nucleation factors are recruited to the Golgi outposts. It has been previously shown that GM130 can recruit AKAP450 to the Golgi complex, but whether the first coiled-coil domain of the *Drosophila* AKAP450 homologue, CP309, can also bind GM130 is unknown (Hurtado et al., 2011; Kawaguchi and Zheng, 2004; Rivero et al., 2009). Interestingly, we observed that predominantly stationary Golgi outposts correlated with EB1 comet formation, indicating that this specific subpopulation may contain γ-tubulin and CP309. What other factors may be necessary to properly position the Golgi outposts at sites such as branchpoints, and how this is achieved will be a fascinating direction for future studies.

Whether the acentrosomal microtubule nucleation uncovered in our study also occurs in the dendrites of mammalian neurons is a question of great interest. Golgi outpost distribution in cultured hippocampal neurons is significantly different than that in da neurons (Horton et al., 2005; Ye et al., 2007), and hippocampal neurons do not form as elaborate arbors as da neurons. However, other types of mammalian neurons form much more complex dendritic arbors and may conceivably require acentrosomal nucleation for the growth and perpetuation of the dendrite branches.

Our study provides the first evidence that Golgi outposts can nucleate microtubules at acentrosomal sites in neurons, shedding new light on the longstanding question about the origin of the microtubule polymer in elongated neuronal processes. This source of nucleation contributes to the complex organization of microtubules within all branches of the neuron, but is specifically necessary for terminal branch development. We thus conclude that acentrosomal microtubule nucleation is essential for dendritic branch growth and overall arbor maintenance of class IV da neurons, and that Golgi outposts are important nucleation centers within the dendritic arbor.

EXPERIMENTAL PROCEDURES

Additional details about the materials and methods used for this paper can be found in the Supplemental Experimental Procedures

Fly Stocks

We used Gal4 driver lines *ppk-Gal4* and *Gal4*[477] (Grueber et al., 2007) to drive the expression of *UAS-ManII-mCherry* and *UAS-ManII-eGFP* (Ye et al., 2007) to visualize Golgi outposts, and *UAS-EB1-GFP* (Satoh et al., 2008; Zheng et al., 2008) to visualize the growing plus ends of microtubules in class IV da neurons. We used the reporter line, *ppk-CD4-tdTomato* (Han et al., 2011) to observe the dendrite morphology of class IV da neurons in wild type and mutant backgrounds. The mutant lines *γ-tubulin23C*[(A15-2)] (Stock 7042) and *CP309*[(5)] (Stock 9567), as well as the *UAS-γ-tubulin23C* RNAi line (Stock 31204)

were obtained from the Bloomington Drosophila Stock Center (Department of Biology, Indiana University, Bloomington, IN).

Live Imaging and Analysis

Whole, live third instar larvae were mounted in 90% glycerol under coverslips sealed with grease, and imaged using a Leica SP5 laser scanning confocal microscope. Live imaging and analysis of EB1-GFP were performed as previously described (Zheng et al., 2008).

In Vitro Microtubule Nucleation Assay

The microtubule nucleation solution assays were performed as described with a few modifications (Kollman et al., 2010; Macurek et al., 2008; Mitchison and Kirschner, 1984). GFP-labeled Golgi vesicles were partially purified by membrane flotation through a sucrose step gradient, then incubated with 10 µM tubulin and 1mM GTP at 25° for 15 min, then 29° for 15 min. The solution was spun onto a coverslip, which was immunostained for α-tubulin (monoclonal T9026, Sigma, St. Louis, MO), γ-tubulin (monoclonal GTU88 or polyclonal T3559, Sigma, St. Louis, MO), or CP309 (polyclonal, gift from Yixian Zheng, Carnegie Institute, HHMI, Baltimore, MD).

Statistical Analysis

All statistical tests were performed with two-tailed Student's t-test.

Supplementary Material

Refer to Web version on PubMed Central for supplementary material.

Acknowledgments

References

Ahmad FJ, Echeverri CJ, Vallee RB, Baas PW. Cytoplasmic dynein and dynactin are required for the transport of microtubules into the axon. J Cell Biol. 1998; 140:391–401. [PubMed: 9442114]

Ahmad FJ, Joshi HC, Centonze VE, Baas PW. Inhibition of microtubule nucleation at the neuronal centrosome compromises axon growth. Neuron. 1994; 12:271–280. [PubMed: 8110458]

Ahmad FJ, Yu W, McNally FJ, Baas PW. An essential role for katanin in severing microtubules in the neuron. J Cell Biol. 1999; 145:305–315. [PubMed: 10209026]

Akhmanova A, Hoogenraad CC, Drabek K, Stepanova T, Dortland B, Verkerk T, Vermeulen W, Burgering BM, De Zeeuw CI, Grosveld F, et al. Clasps are CLIP-115 and -170 associating proteins involved in the regional regulation of microtubule dynamics in motile fibroblasts. Cell. 2001; 104:923–935. [PubMed: 11290329]

Baas PW, Deitch JS, Black MM, Banker GA. Polarity orientation of microtubules in hippocampal neurons: uniformity in the axon and nonuniformity in the dendrite. Proc Natl Acad Sci U S A. 1988; 85:8335–8339. [PubMed: 3054884]

Baas PW, Karabay A, Qiang L. Microtubules cut and run. Trends Cell Biol. 2005; 15:518–524. [PubMed: 16126385]

Bartolini F, Gundersen GG. Generation of noncentrosomal microtubule arrays. J Cell Sci. 2006; 119:4155–4163. [PubMed: 17038542]

Basto R, Lau J, Vinogradova T, Gardiol A, Woods CG, Khodjakov A, Raff JW. Flies without centrioles. Cell. 2006; 125:1375–1386. [PubMed: 16814722]

Chabin-Brion K, Marceiller J, Perez F, Settegrana C, Drechou A, Durand G, Pous C. The Golgi complex is a microtubule-organizing organelle. Mol Biol Cell. 2001; 12:2047–2060. [PubMed: 11452002]

Desai A, Mitchison TJ. Microtubule polymerization dynamics. Annu Rev Cell Dev Biol. 1997; 13:83–117. [PubMed: 9442869]

Efimov A, Kharitonov A, Efimova N, Loncarek J, Miller PM, Andreyeva N, Gleeson P, Galjart N, Maia AR, McLeod IX, et al. Asymmetric CLASP-dependent nucleation of noncentrosomal microtubules at the trans-Golgi network. Dev Cell. 2007; 12:917–930. [PubMed: 17543864]

Ferreira A, Palazzo RE, Rebhun LI. Preferential dendritic localization of pericentriolar material in hippocampal pyramidal neurons in culture. Cell Motil Cytoskeleton. 1993; 25:336–344. [PubMed: 8402954]

Gardiol A, Racca C, Triller A. Dendritic and postsynaptic protein synthetic machinery. J Neurosci. 1999; 19:168–179. [PubMed: 9870948]

Grueber WB, Jan LY, Jan YN. Tiling of the Drosophila epidermis by multidendritic sensory neurons. Development. 2002; 129:2867–2878. [PubMed: 12050135]

Grueber WB, Jan LY, Jan YN. Different levels of the homeodomain protein cut regulate distinct dendrite branching patterns of Drosophila multidendritic neurons. Cell. 2003; 112:805–818. [PubMed: 12654247]

Grueber WB, Ye B, Yang CH, Younger S, Borden K, Jan LY, Jan YN. Projections of Drosophila multidendritic neurons in the central nervous system: links with peripheral dendrite morphology. Development. 2007; 134:55–64. [PubMed: 17164414]

Han C, Jan LY, Jan YN. Enhancer-driven membrane markers for analysis of nonautonomous mechanisms reveal neuron-glia interactions in Drosophila. Proc Natl Acad Sci U S A. 2011; 108:9673–9678. [PubMed: 21606367]

Han C, Wang D, Soba P, Zhu S, Lin X, Jan LY, Jan YN. Integrins regulate repulsion-mediated dendritic patterning of drosophila sensory neurons by restricting dendrites in a 2D space. Neuron. 2012; 73:64–78. [PubMed: 22243747]

Hendricks AG, Perlson E, Ross JL, Schroeder HW 3rd, Tokito M, Holzbaur EL. Motor Coordination via a Tug-of-War Mechanism Drives Bidirectional Vesicle Transport. Curr Biol. 2010; 20:697–702. [PubMed: 20399099]

Hoogenraad CC, Bradke F. Control of neuronal polarity and plasticity--a renaissance for microtubules? Trends Cell Biol. 2009; 19:669–676. [PubMed: 19801190]

Horton AC, Ehlers MD. Dual modes of endoplasmic reticulum-to-Golgi transport in dendrites revealed by live-cell imaging. J Neurosci. 2003; 23:6188–6199. [PubMed: 12867502]

Horton AC, Racz B, Monson EE, Lin AL, Weinberg RJ, Ehlers MD. Polarized secretory trafficking directs cargo for asymmetric dendrite growth and morphogenesis. Neuron. 2005; 48:757–771. [PubMed: 16337914]

Hurtado L, Caballero C, Gavilan MP, Cardenas J, Bornens M, Rios RM. Disconnecting the Golgi ribbon from the centrosome prevents directional cell migration and ciliogenesis. J Cell Biol. 2011; 193:917–933. [PubMed: 21606206]

Jaworski J, Kapitein LC, Gouveia SM, Dortland BR, Wulf PS, Grigoriev I, Camera P, Spangler SA, Di Stefano P, Demmers J, et al. Dynamic microtubules regulate dendritic spine morphology and synaptic plasticity. Neuron. 2009; 61:85–100. [PubMed: 19146815]

Jinushi-Nakao S, Arvind R, Amikura R, Kinameri E, Liu AW, Moore AW. Knot/Collier and cut control different aspects of dendrite cytoskeleton and synergize to define final arbor shape. Neuron. 2007; 56:963–978. [PubMed: 18093520]

Joshi HC, Palacios MJ, McNamara L, Cleveland DW. Gamma-tubulin is a centrosomal protein required for cell cycle-dependent microtubule nucleation. Nature. 1992; 356:80–83. [PubMed: 1538786]

Kapitein LC, Schlager MA, Kuijpers M, Wulf PS, van Spronsen M, MacKintosh FC, Hoogenraad CC. Mixed microtubules steer dynein-driven cargo transport into dendrites. Curr Biol. 2010; 20:290–299. [PubMed: 20137950]

Kawaguchi S, Zheng Y. Characterization of a Drosophila centrosome protein CP309 that shares homology with Kendrin and CG-NAP. Mol Biol Cell. 2004; 15:37–45. [PubMed: 14565985]

Keating TJ, Borisy GG. Centrosomal and non-centrosomal microtubules. Biol Cell. 1999; 91:321–329. [PubMed: 10518998]

Kollman JM, Polka JK, Zelter A, Davis TN, Agard DA. Microtubule nucleating gamma-TuSC assembles structures with 13-fold microtubule-like symmetry. Nature. 2010; 466:879–882. [PubMed: 20631709]

Lee SB, Bagley JA, Lee HY, Jan LY, Jan YN. Pathogenic polyglutamine proteins cause dendrite defects associated with specific actin cytoskeletal alterations in Drosophila. Proc Natl Acad Sci U S A. 2011; 108:16795–16800. [PubMed: 21930920]

Macurek L, Draberova E, Richterova V, Sulimenko V, Sulimenko T, Draberova L, Markova V, Draber P. Regulation of microtubule nucleation from membranes by complexes of membrane-bound gamma-tubulin with Fyn kinase and phosphoinositide 3-kinase. Biochem J. 2008; 416:421–430. [PubMed: 18636972]

Mattie FJ, Stackpole MM, Stone MC, Clippard JR, Rudnick DA, Qiu Y, Tao J, Allender DL, Parmar M, Rolls MM. Directed microtubule growth, +TIPs, and kinesin-2 are required for uniform microtubule polarity in dendrites. Curr Biol. 2010; 20:2169–2177. [PubMed: 21145742]

Miller PM, Folkmann AW, Maia AR, Efimova N, Efimov A, Kaverina I. Golgi-derived CLASP-dependent microtubules control Golgi organization and polarized trafficking in motile cells. Nat Cell Biol. 2009; 11:1069–1080. [PubMed: 19701196]

Mitchison T, Kirschner M. Dynamic instability of microtubule growth. Nature. 1984; 312:237–242. [PubMed: 6504138]

Nguyen MM, Stone MC, Rolls MM. Microtubules are organized independently of the centrosome in Drosophila neurons. Neural Dev. 2011; 6:38. [PubMed: 22145670]

Oakley BR. gamma-Tubulin. Curr Top Dev Biol. 2000; 49:27–54. [PubMed: 11005013]

Oegema K, Wiese C, Martin OC, Milligan RA, Iwamatsu A, Mitchison TJ, Zheng Y. Characterization of two related Drosophila gamma-tubulin complexes that differ in their ability to nucleate microtubules. J Cell Biol. 1999; 144:721–733. [PubMed: 10037793]

Ori-McKenney KM, Xu J, Gross SP, Vallee RB. A cytoplasmic dynein tail mutation impairs motor processivity. Nat Cell Biol. 2010; 12:1228–1234. [PubMed: 21102439]

Parrish JZ, Xu P, Kim CC, Jan LY, Jan YN. The microRNA bantam functions in epithelial cells to regulate scaling growth of dendrite arbors in drosophila sensory neurons. Neuron. 2009; 63:788–802. [PubMed: 19778508]

Pierce JP, Mayer T, McCarthy JB. Evidence for a satellite secretory pathway in neuronal dendritic spines. Curr Biol. 2001; 11:351–355. [PubMed: 11267872]

Rivero S, Cardenas J, Bornens M, Rios RM. Microtubule nucleation at the cis-side of the Golgi apparatus requires AKAP450 and GM130. EMBO J. 2009; 28:1016–1028. [PubMed: 19242490]

Rogers GC, Rusan NM, Peifer M, Rogers SL. A multicomponent assembly pathway contributes to the formation of acentrosomal microtubule arrays in interphase Drosophila cells. Mol Biol Cell. 2008; 19:3163–3178. [PubMed: 18463166]

Rolls MM, Satoh D, Clyne PJ, Henner AL, Uemura T, Doe CQ. Polarity and intracellular compartmentalization of Drosophila neurons. Neural Dev. 2007; 2:7. [PubMed: 17470283]

Satoh D, Sato D, Tsuyama T, Saito M, Ohkura H, Rolls MM, Ishikawa F, Uemura T. Spatial control of branching within dendritic arbors by dynein-dependent transport of Rab5-endosomes. Nat Cell Biol. 2008; 10:1164–1171. [PubMed: 18758452]

Song Y, Ori-McKenney KM, Zheng Y, Han C, Jan LY, Jan YN. Regeneration of Drosophila sensory neuron axons and dendrites is regulated by the Akt pathway involving Pten and microRNA bantam. Genes Dev. 2012; 26:1612–1625. [PubMed: 22759636]

Stepanova T, Slemmer J, Hoogenraad CC, Lansbergen G, Dortland B, De Zeeuw CI, Grosveld F, van Cappellen G, Akhmanova A, Galjart N. Visualization of microtubule growth in cultured neurons via the use of EB3-GFP (end-binding protein 3-green fluorescent protein). J Neurosci. 2003; 23:2655–2664. [PubMed: 12684451]

Stewart A, Tsubouchi A, Rolls MM, Tracey WD, Sherwood NT. Katanin p60-like1 Promotes Microtubule Growth and Terminal Dendrite Stability in the Larval Class IV Sensory Neurons of Drosophila. J Neurosci. 2012; 32:11631–11642. [PubMed: 22915107]

Stiess M, Bradke F. Neuronal polarization: The cytoskeleton leads the way. Dev Neurobiol. 2010

Stiess M, Maghelli N, Kapitein LC, Gomis-Ruth S, Wilsch-Brauninger M, Hoogenraad CC, Tolic-Norrelykke IM, Bradke F. Axon extension occurs independently of centrosomal microtubule nucleation. Science. 2010; 327:704–707. [PubMed: 20056854]

Stone MC, Roegiers F, Rolls MM. Microtubules have opposite orientation in axons and dendrites of Drosophila neurons. Mol Biol Cell. 2008; 19:4122–4129. [PubMed: 18667536]

Wang L, Brown A. Rapid movement of microtubules in axons. Curr Biol. 2002; 12:1496–1501. [PubMed: 12225664]

Wiese C, Zheng Y. Microtubule nucleation: gamma-tubulin and beyond. J Cell Sci. 2006; 119:4143–4153. [PubMed: 17038541]

Witte H, Bradke F. The role of the cytoskeleton during neuronal polarization. Curr Opin Neurobiol. 2008; 18:479–487. [PubMed: 18929658]

Ye B, Zhang Y, Song W, Younger SH, Jan LY, Jan YN. Growing dendrites and axons differ in their reliance on the secretory pathway. Cell. 2007; 130:717–729. [PubMed: 17719548]

Yu W, Centonze VE, Ahmad FJ, Baas PW. Microtubule nucleation and release from the neuronal centrosome. J Cell Biol. 1993; 122:349–359. [PubMed: 8320258]

Yu W, Qiang L, Solowska JM, Karabay A, Korulu S, Baas PW. The microtubule-severing proteins spastin and katanin participate differently in the formation of axonal branches. Mol Biol Cell. 2008; 19:1485–1498. [PubMed: 18234839]

Zheng Y, Wildonger J, Ye B, Zhang Y, Kita A, Younger SH, Zimmerman S, Jan LY, Jan YN. Dynein is required for polarized dendritic transport and uniform microtubule orientation in axons. Nat Cell Biol. 2008; 10:1172–1180. [PubMed: 18758451]
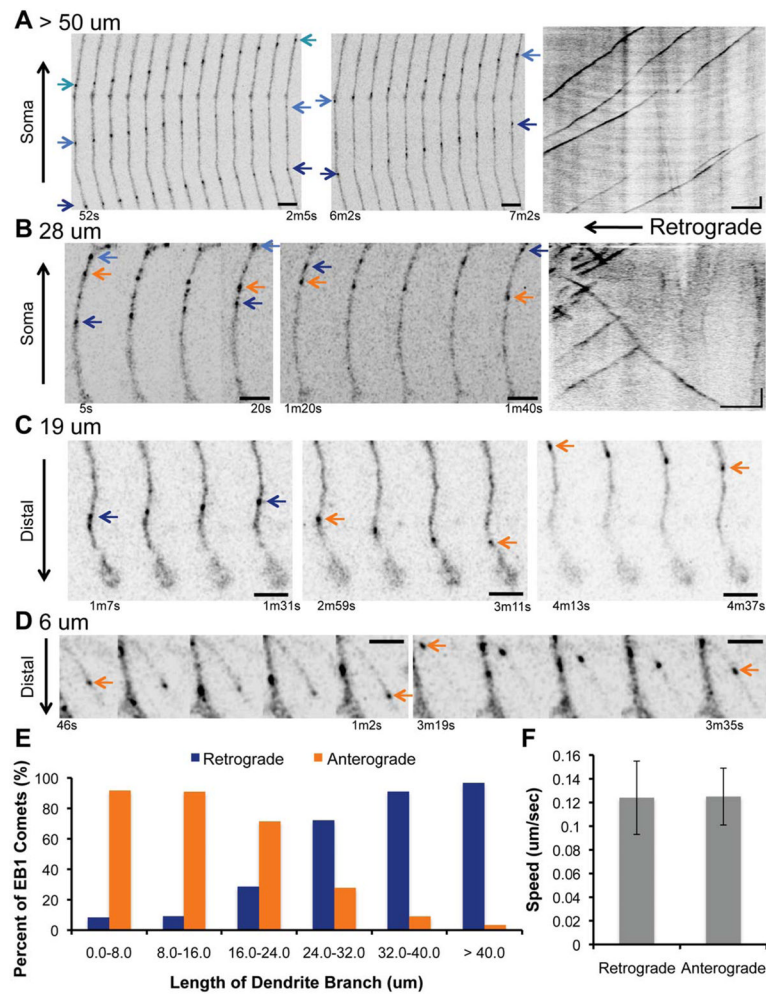
Figure 1. Microtubule orientation correlates with dendrite branch length in class IV dendritic arborization neurons
Movie montages and/or kymographs depict the trajectory of EB1-GFP comets in dendrite processes that are > 50 μm (**A**), 28 μm (**B**), 19 μm (**C**), or 6 μm (**D**) (See Figure S1 for branch classification). Black arrows indicate the direction of the soma or distal tip for each montage. *UAS-EB1-GFP* was expressed in class IV neurons by *ppk-Gal4*. In long primary branches, the majority of the comets move retrogradely towards the cell body, but in shorter terminal branches, most of the comets move anterogradely towards the distal tip of the process. Blue and orange arrows indicate the starting and ending positions of comets growing retrogradely or anterogradely, respectively. Montage scale bars are 3 μm for (**A**) and (**B**) and 2.5 μm for (**C**) and (**D**). Kymograph scale bars are 5 μm (x axis) and 30 s (y axis). (**E**) Histogram revealing the correlation between EB1-GFP comet directionality and length of the dendrite branch. Longer branches contain predominantly retrogradely moving comets, while shorter branches frequently possess anterogradely moving comets. $N = 14$ neurons with 71 anterograde and 62 retrograde comets. (**F**) Bar graph showing comparable speeds (means ± s.d.) for retrograde and anterograde EB1-GFP comets ($P = .799$; $n = 44$ neurons and 204 comets).
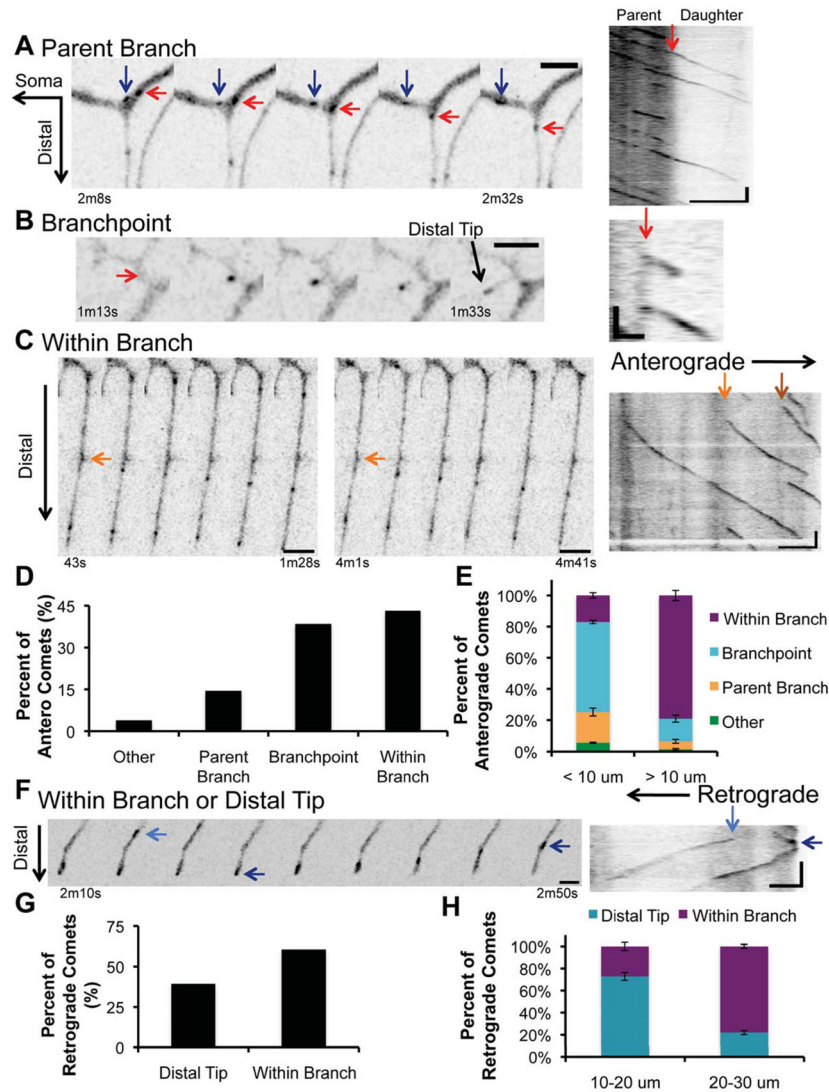
Figure 2. Anterograde and retrograde comets originate from specific sites within the dendritic arbor

EB1-GFP comets growing anterogradely into a branch primarily originate from one of three sources: a parent branch, within the branch, or a branchpoint. Black arrows indicate the direction of the soma or distal tip for each montage. (**A**) EB1-GFP comets can be directed from the parent branch into a smaller branch. The red arrow identifies a comet that is guided into the smaller daughter branch from the parent branch, while the blue arrow follows a comet that bypasses the daughter branch. The red arrow in the corresponding kymograph indicates the point at which three comets are directed into the daughter branch. (**B**) Anterograde comets can originate from a specific branchpoint structure of a nascent branch. Red arrows indicate the branchpoint site of nucleation in both the montage and kymograph. (**C**) Anterograde comets originating within a branch also grow from specific sites (See also Movie S1). The orange arrows point to the identical origin of multiple EB1 comets. (**D**) and (**E**) Bar graphs depicting the percent of total anterograde comets that originate from each source, and that the source of EB1 comets for a branch depends on its length. (**F**) Retrograde EB1-GFP comets growing from a terminal branch originate from one of two sources: within the branch or from the distal tip (light and dark blue arrows, respectively in the montage and

kymograph) (See also Figure S2). (**G**) and (**H**) Bar graphs depicting the percent of total retrograde comets that originate from each source, and that the source of EB1 comets for a branch depends on its length. Montage scale bars are 3 μm. Kymograph scale bars are 5 μm (x axis) and 30 s (y axis) for (**A**) and (**C**), 1.5 μm and 20 s for (**B**), and 2 μm and 30 s for (**F**). Data are means ± s.e.m.; n = 26 neurons and 133 comets for anterograde quantification and 21 neurons and 50 comets for retrograde quantification.
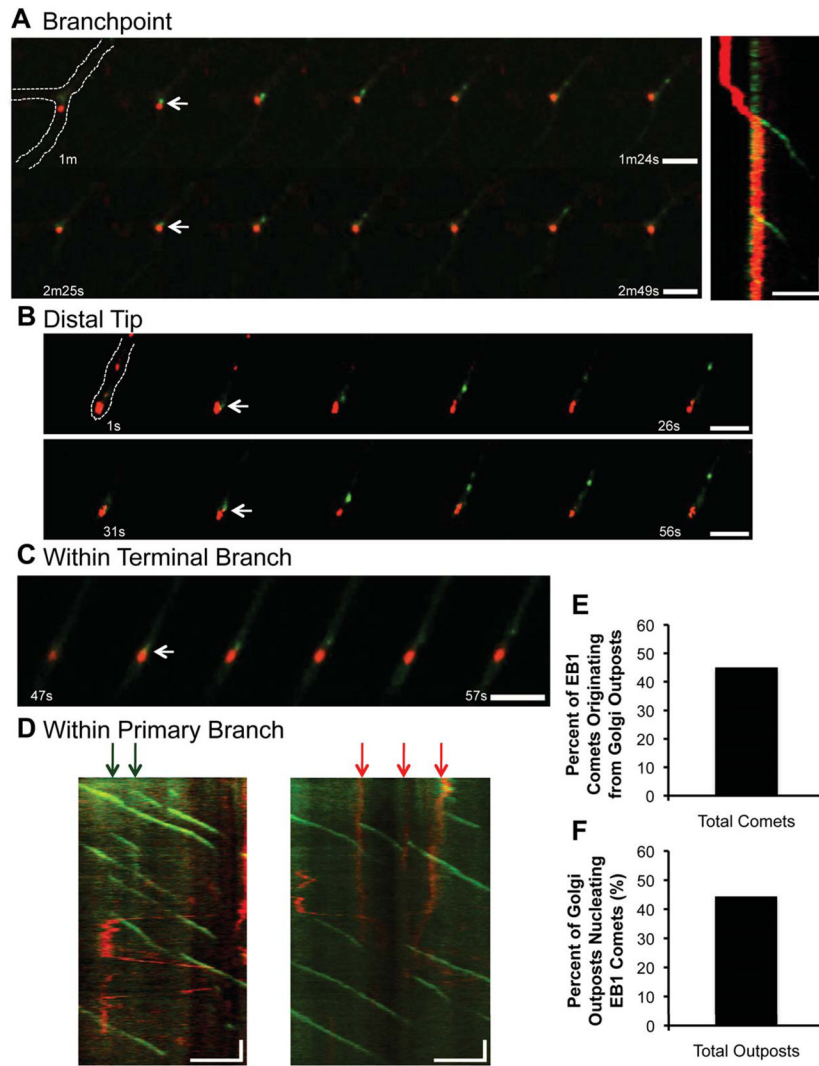
Figure 3. Golgi outposts colocalize with sites of EB1-GFP comet formation *in vivo*
EB1-GFP comets emanate from Golgi outposts at branchpoints (**A**), distal tips (**B**), and
within the terminal branches (**C**) of class IV da neurons (See also Movie S2). *UAS-EB1-
GFP* and *UAS-ManII-mCherry* were expressed in class IV neurons by *Gal4[4-77]*. White
arrows indicate the generation of EB1 comets (green) at the location of Golgi outposts (red).
(**D**) EB1 comets also originate from Golgi outposts within primary branches. In the
kymographs, red arrows indicate the generation of EB1 comets (green) at stationary Golgi
outposts (red), while green arrows indicate the EB1 comets that are not generated at Golgi
outposts. Montage scale bars are 3 μm. Kymograph scale bars are 5 μm (x axis) and 30 s (y
axis). (**E**) and (**F**) Bar graphs showing the total percent of Golgi outposts that colocalize
with sites of EB1 comet formation and the total percent of EB1 comets that originate from
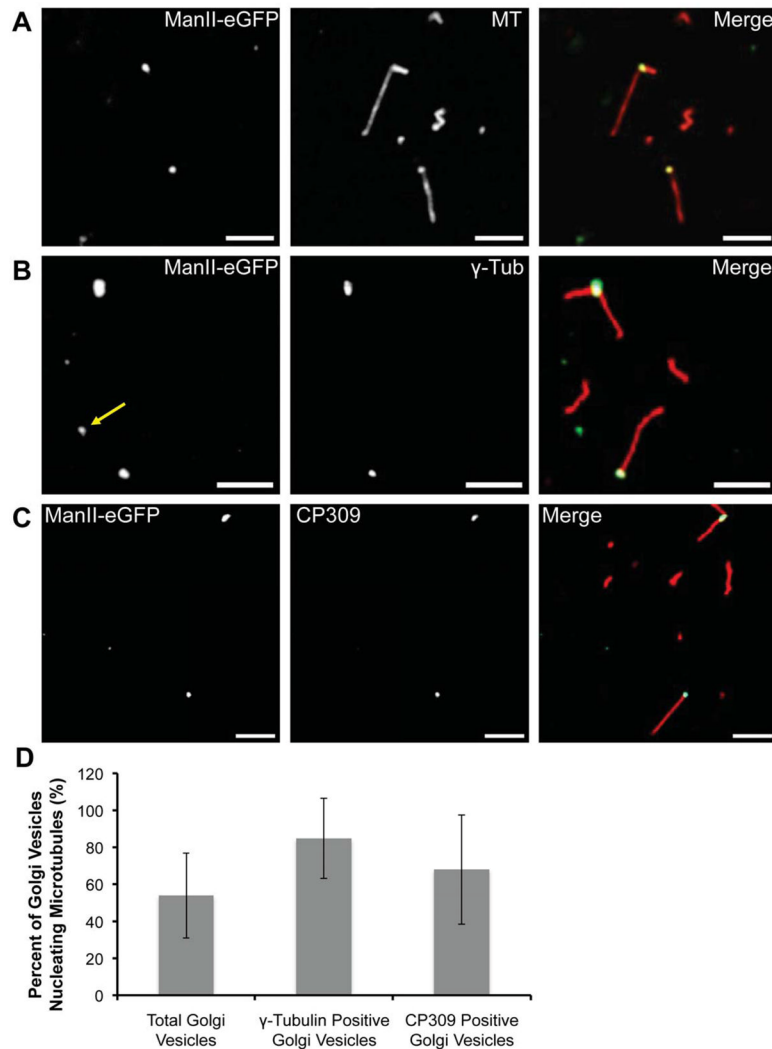Golgi structures *in vivo*, $n = 26$ neurons. See also Figure S3.

Figure 4. Golgi vesicles promote microtubule nucleation *in vitro*
Golgi vesicles were partially purified from *ppk-Gal4>UAS-ManII-eGFP* embryo lysate by membrane flotation, then incubated with 10 μM tubulin and 1 mM GTP at 25°C for 15 min., then 29°C for 15 min. After fixation, samples were centrifuged onto coverslips, which were used for immunostaining. (**A**) Multiple microtubules (MT) extend from ManII-eGFP Golgi structures. (**B**) and (**C**) Golgi vesicles that nucleate microtubules are positive for γ-tubulin and CP309. Yellow arrow points to a vesicle negative for γ-tubulin that is not associated with microtubules. (**D**) Bar graph showing the percent of total Golgi vesicles that nucleate microtubules *in vitro* and the percent of γ-tubulin and CP309 positive vesicles that nucleate microtubules *in vitro*. Data are means ± s.d.; *n* = 5, 3, and 3 experiments for (**A**), (**B**), and (**C**), respectively. Scale bars are 5 μm. See also Figure S4.
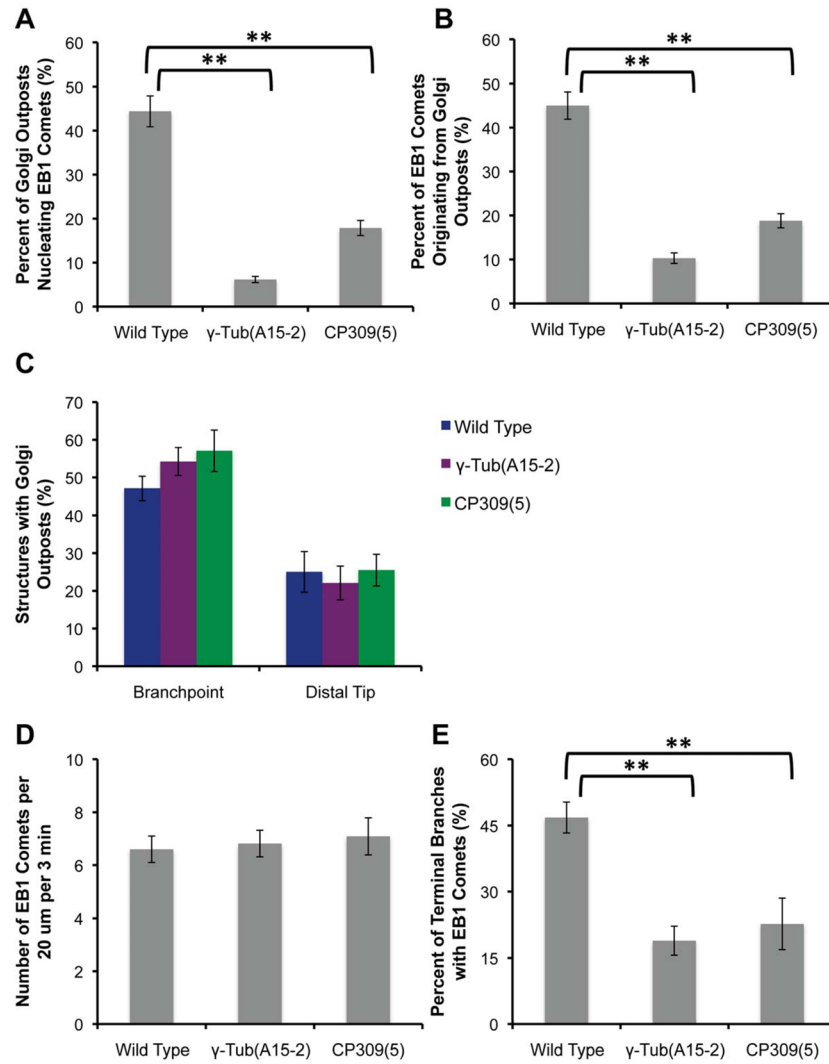
Figure 5. Golgi-dependent microtubule nucleation requires γ-tubulin and CP309
The percent of Golgi outposts that colocalize with EB1 comets and the percent of EB1 comets that emanate from Golgi outposts *in vivo* is dramatically decreased in *γ-tubulin23C RNAi/γ-tubulin23C(A15-2)* and *CP309(5)/CP309(5)* mutant larval neurons as shown in (**A**) and (**B**). Data are means ± s.e.m.; n = 93, 96, and 93 Golgi outposts and n = 127, 99, and 115 EB1 comets for wild type, γ-tubulin mutant, and CP309 mutant, respectively. Stars indicate P < 0.001. (**C**) Bar graph revealing a similar percent of branchpoints and distal tips that contain Golgi outposts throughout the arbors of wild type, *γ-tubulin23C RNAi/γ-tubulin23C(A15-2)* and *CP309(5)/CP309(5)* mutant neurons. Data are means ± s.e.m.; n = 22, 10, and 10 neurons for wild type, γ-tubulin mutant, and CP309 mutant, respectively. (**D**)-(**E**) Bar graphs showing that although there are a similar number of EB1-GFP comets in the primary branches of *γ-tubulin23C RNAi/γ-tubulin23C(A15-2)* and *CP309(5)/CP309(5)* mutant neurons compared with wild type, there is a dramatic reduction in the percent of terminal branches that have EB1-GFP comets. Data are means ± s.e.m.; n = 11, 11, and 10 neurons for (**D**) and n = 20, 15, and 15 neurons for (**E**) for wild type, γ-tubulin mutant, and CP309 mutant, respectively. Stars indicate P < 0.001.
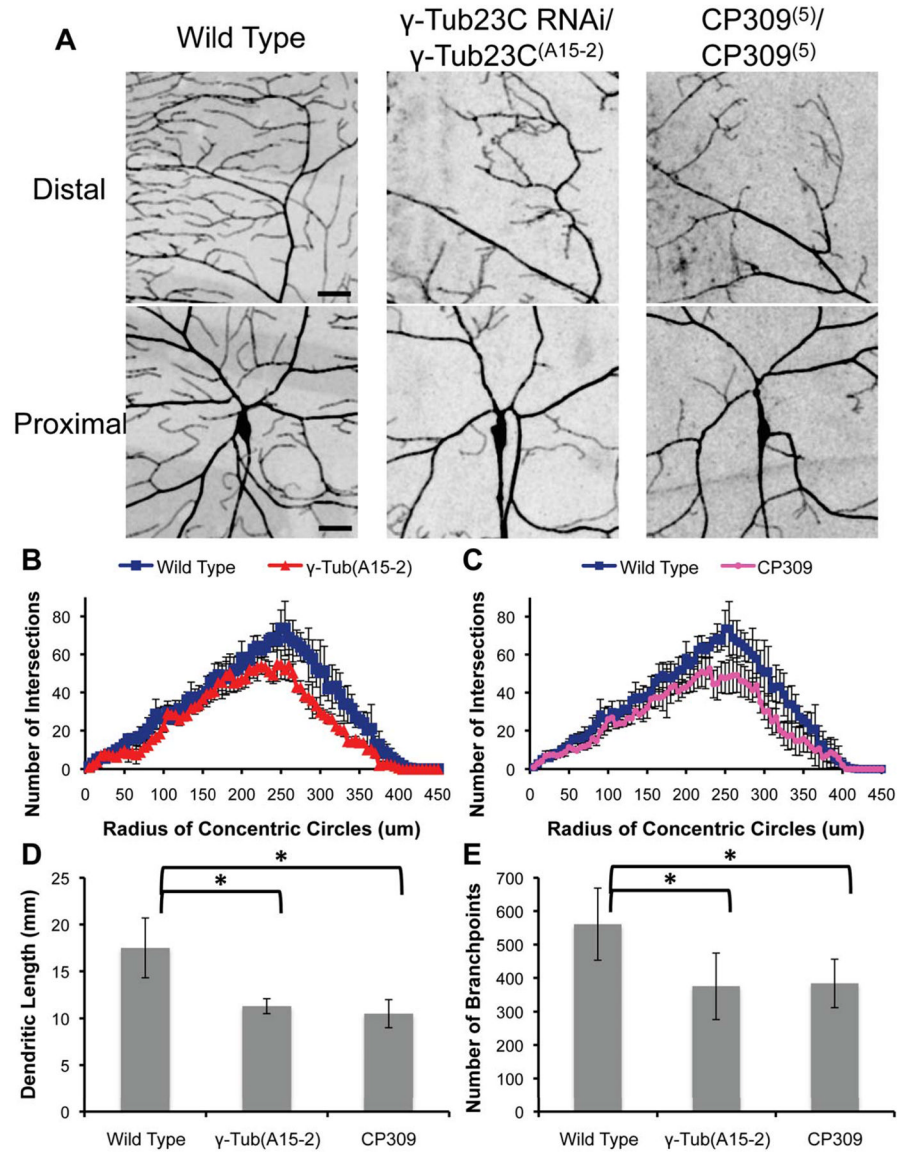
Figure 6. Loss of γ-tubulin or CP309 function alters the dendritic morphology of class IV da neurons

(**A**) Dendrite defects in *γ-tubulin23C RNAi/γ-tubulin23C(A15-2)* and *CP309(5)/CP309(5)* mutant class IV da neurons, visualized by *ppk-cd4-tdtom*. Scale bars are 25 μm. (**B**) and (**C**) Sholl analysis reveals decreased complexity of the dendritic arbor in the absence of γ-tubulin or CP309. Data are means ± s.d.; *n* = 4 neurons per genotype. (**D**) and (**E**) Total dendrite length and number of branchpoints were reduced in *γ-tubulin23C RNAi/γ-tubulin23C(A15-2)* and *CP309(5)/CP309(5)* mutant neurons. Data are means ± s.d.; *n* = 4 neurons per genotype. Stars indicate *P* < 0.05.
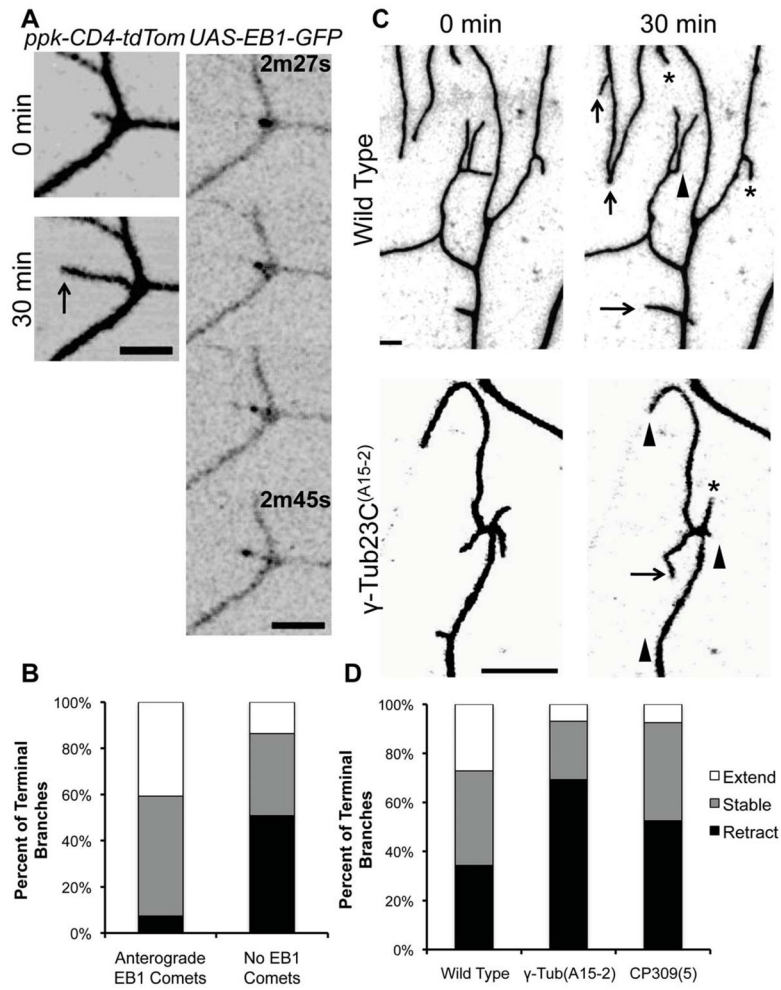
Figure 7. Microtubule dynamics are important for dendrite branch extension and stability
(**A**) Movie montage shows EB1 comets grow into branches that extend and remain stable in a wild type neuron (arrow indicates point of branch extension within 30 min) (See also Figure S5). (**B**) Quantification of the correlation between EB1 comet growth within a branch and branch dynamics; n = 86 branches. (**C**) Representative images of dendrite branch dynamics in wild type or γ-tubulin23C RNAi/γ-tubulin23C$^{(A15-2)}$ neurons within 30 min. Arrows, arrowheads, and stars indicate points of branch extension, retraction, and stability after 30 min for each genotype. (**D**) Quantification of total branch dynamics in wild type, γ-tubulin23C RNAi/γ-tubulin23C$^{(A15-2)}$ and CP309$^{(5)}$/CP309$^{(5)}$ neurons. N = 96, 101, and 120 branches for wild type, γ-tubulin mutant, and CP309 mutant, respectively.